Hindawi Publishing Corporation
Advances in Condensed Matter Physics
Volume 2012, Article ID 281371, 13 pages
doi:10.1155/2012/281371

Research Article

Gap Structure and Gapless Structure in Fractional Quantum Hall Effect

Shosuke Sasaki

KYOKUGEN (Center for Quantum Science and Technology under Extreme Conditions), Osaka University, 1-3 Machikaneyama, Toyonaka, Osaka 560-8531, Japan

Correspondence should be addressed to Shosuke Sasaki, sasaki@ns.sist.ac.jp

Received 14 November 2011; Revised 9 January 2012; Accepted 24 January 2012

Academic Editor: Roberto Zivieri

Higher-order composite fermion states are correlated with many quasiparticles. The energy calculations are very complicated. We develop the theory of Tao and Thouless to explain them. The total Hamiltonian is $(H_D + H_I)$, where H_D includes Landau energies and classical Coulomb energies. We find the most uniform electron configuration in Landau states which has the minimum energy of H_D. At $\nu = (2j-1)/(2j)$, all the nearest electron pairs are forbidden to transfer to any empty states because of momentum conservation. Therefore, perturbation energies of the nearest electron pairs are zero in all order of perturbation. At $\nu = j/(2j-1)$, $j/(2j+1)$, all the nearest electron (or hole) pairs can transfer to all hole (or electron) states. At $\nu = 4/11, 4/13, 5/13, 5/17, 6/17$, only the specific nearest hole pairs can transfer to all electron states. For example, the nearest-hole-pair energy at $\nu = 4/11$ is lower than the limiting energies from both sides (the left side $\nu = (4s+1)/(11s+3)$ and the right side $\nu = (4s-1)/(11s-3)$ for infinitely large s). Thus, the nearest-hole-pair energy at specific ν is different from the limiting values from both sides. The property yields energy gap for the specific ν. Also gapless structure appears at other filling factors (e.g., at $\nu = 1/2$).

1. Introduction

Precise experiments on ultra-high-mobility samples revealed many local minima of diagonal resistivity ρ_{xx} [1, 2]. Therein small local minima are detected at the filling factors of $\nu = 3/8, 3/10, 7/11, 4/11, 4/13, 5/13, 5/17$, and $6/17,\ldots$. These states cannot be understood by use of the standard composite fermion (CF) model [3, 4]. Jain has originally considered multiflavor composite fermion picture with coexistence of composite fermions carrying different numbers of fluxes. Wójs et al. [5, 6], Smet [7], and Peterson and Jain [8] and Pashitskii [9] investigated these states and described the states in their extended systematics. Smet has explained these states in terms of the multiflavor composite fermion picture. Pashitskii presented expanded systematics based on Halperin's conjecture of coexistence of free electrons and bound electron pairs, with predicted new exotic fractions of $\nu = 5/14, 5/16$, and $3/20$. These investigations are complicated to explain the stability of expanded states with $\nu = 3/8, 3/10, 7/11, 4/11, 4/13, 5/13, 5/17$, and $6/17,\ldots$, because many quasiparticles are correlated with each others. The results of various theories depend upon what kinds of quasi-particles are combined with each others. Therefore, it is preferable that the same logic is applied to any kind of filling factors (including both standard and nonstandard filling factors).

We study the other description in order to remove these ambiguities. Tao and Thouless [10, 11] examined the case that the lowest Landau levels are partially filled with electrons. They cannot lead which states are stable in comparison with the other states. However, their method is very important to investigate the FQH states. We have carefully examined the Coulomb interactions and develop their theory [12, 13]. Then the Coulomb transitions conserve the x component of the total momentum where the x direction indicates the current direction. This property produces energy gaps for the specific filling factors. Also the momentum conservation produces no binding energy for some filling factors. We study these gap structure or gapless structure for various filling factors, respectively. Quantum hall devices have an ultra thin layer of electron conducting channel as in Figure 1.

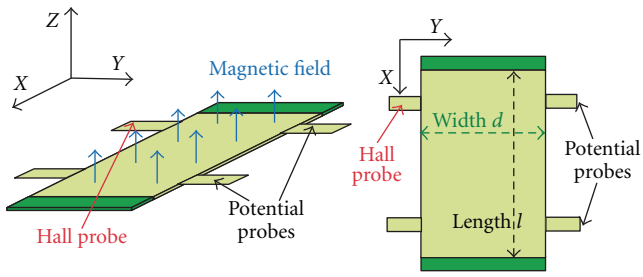

FIGURE 1: Quantum hall device.

That is to say the potential well in the z direction is deep and extremely narrow. Then the electron state of the z-direction is the ground state $\phi(z)$ at a low temperature because the probability of excited states is negligibly small caused by large excitation energy. The remaining freedoms are the x and y directions. If we neglect the Coulomb interactions between electrons, the single-electron eigenstates are the Landau states. Although these states are well known, we shortly write them for applying them below. Landau wave function is given as follows:

$$\psi_{L,J}(x,y,z) = \sqrt{\frac{1}{\ell}}\exp(ikx)u_L H_L\left(\sqrt{\frac{m\omega}{\hbar}}(y-\alpha_J)\right) \times \exp\left(-\frac{m\omega}{2\hbar}(y-\alpha_J)^2\right)\phi(z). \tag{1}$$

Therein, L is the Landau level number, k is the angular wavenumber, and α_J is the central position in the y-direction which is related as

$$\alpha_J = \frac{2\pi\hbar J}{(eB\ell)} \qquad k = \frac{2\pi J}{\ell}, \tag{2}$$

where J indicates the integer assigned to each momentum of the x-direction. The eigen energy is

$$E_L = \lambda + \hbar\omega\left(L+\frac{1}{2}\right) \quad (L = 0,1,2,3,\ldots), \tag{3}$$

where λ is the ground state energy of the z-direction. We count the number of states with a fixed value of L by (2)

$$0 \le \alpha_J \le d \longrightarrow 0 \le \frac{2\pi\hbar J}{(eB\ell)} \le d \longrightarrow 0 \le J \le \frac{eB\ell d}{(2\pi\hbar)}, \tag{4}$$

where d is the width of the device in Figure 1. Then the total number of Landau states with the same value of L is equal to $eB\ell d/(2\pi\hbar)$.

Next we consider the many electron states $\Psi(L_1,\ldots,L_N; p_1,\ldots,p_N)$ described by the Slater determinant where L_j and p_j indicate the Landau level number and the momentum of jth electron, respectively. All the states composed of $\Psi(L_1,\ldots,L_N; p_1,\ldots,p_N)$ make the complete set. The total Hamiltonian is rewritten by use of this complete set. The diagonal part is described by H_D which is given as

$$H_D = \sum_{L_1,\ldots,L_N}\sum_{p_1,\ldots,p_N} |\Psi(L_1,\ldots,L_N; p_1,\ldots,p_N)\rangle \times W(L_1,\ldots,L_N; p_1,\ldots,p_N) \times \langle\Psi(L_1,\ldots,L_N; p_1,\ldots,p_N)|, \tag{5}$$

where $W(L_1,\ldots,L_N; p_1,\ldots,p_N)$ is the diagonal matrix element defined by

$$W(L_1,\ldots,L_N; p_1,\ldots,p_N) = \sum_{i=1}^{N} E_{L_i} + C(L_1,\ldots,L_N; p_1,\ldots,p_N). \tag{6}$$

Therein, E_{L_i} is the eigen-energy (3) of single electron with Landau level number L_i. Also C is the expectation value of Coulomb interactions which is defined by

$$C(L_1,\ldots,L_N; p_1,\ldots,p_N) = \int\cdots\int \Psi(L_1,\ldots,L_N; p_1,\ldots,p_N)^* \times \sum_{i=1}^{N-1}\sum_{j>i}^{N} \frac{e^2}{4\pi\varepsilon\sqrt{(x_i-x_j)^2+(y_i-y_j)^2+(z_i-z_j)^2}} \times \Psi(L_1,\ldots,L_N; p_1,\ldots,p_N) \times dx_1 dy_1 dz_1 \cdots dx_N dy_N dz_N. \tag{7}$$

Hereafter, we call $C(L_1,\ldots,L_N; p_1,\ldots,p_N)$ "classical Coulomb energy." The total Hamiltonian is divided into two parts H_D and H_I. The residual part H_I is obtained by

$$H_I = H_T - H_D, \tag{8}$$

where H_I is constructed only by the off-diagonal elements. The residual Hamiltonian H_I is the interaction between two electrons depending upon only the relative coordinate. Therefore, the total momentum of the x-direction conserves in this system. That is to say the sum of the initial momenta p_i and p_j is equal to the sum of the final momenta p_i' and p_j' via Coulomb transition as follows:

$$p_i' + p_j' = p_i + p_j. \tag{9}$$

At a filling factor smaller than 1, the ground state of H_D is the following many-electron state as:

(1) N electrons exist in the lowest Landau levels of $L_1 = L_2 = \cdots = L_N = 0$.

(2) The electrons should most uniformly occupy the lowest Landau levels so that the classical Coulomb energy has the lowest value. The electron momenta $p_1, p_2, \ldots p_N$ are related to each centre positions as in (2). Therefore, the most uniform electron configuration determines the electron momenta $p_1, p_2, \ldots, p_N$ for each filling factor ν.

In the next section we will schematically draw the most uniform electron configuration at several filling factors. Then it is clarified that the most uniform electron configuration is unique. The most uniformity yields the minimum eigen energy of H_D, and the uniqueness produces a nondegenerate ground state although the ground states of the single electron Hamiltonian H_0 are degenerate. The electron configurations are examined in Section 2.

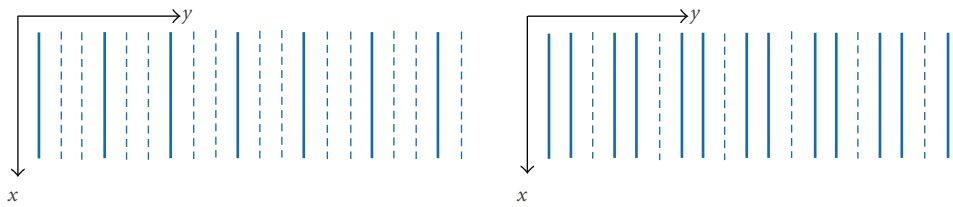

Figure 2: (a) Electron configuration at $\nu = 1/3$. (b) Configuration at $\nu = 2/3$.

We can estimate the perturbation energy via the Coulomb transitions by using the usual perturbation method of nondegenerate case. Electron (or hole) pairs in the nearest Landau orbitals are most affected by the Coulomb interaction. The perturbation energies of the nearest electron (or hole) pairs are sensitively dependent upon each electron configurations. The sensitivity is caused by Fermi-Dirac statistics and the momentum conservation of the x-direction. The most uniform electron configuration produces the following properties: all the *nearest electron* (or *hole*) *pairs* are allowed to transfer to all vacant (or filled) states at the filling factors of $\nu = j/(2j \pm 1)$. The property produces energy gap structure. For example, the perturbation energy of the *nearest electron pair* at $\nu = j/(2j-1)$ is lower than the limiting value from both sides as $s \to \nu \pm \varepsilon$ where ε is an infinitesimally small value. The energy gap is defined as

$$\text{Energy gap} = \Delta E_{\text{nearest pair}} = \left(E(\nu) - \lim_{s \to \nu+\varepsilon} E(s)\right). \quad (10)$$

The ratio of the energy gap and the original nearest electron pair energy is equal to

$$\frac{\Delta E_{\text{nearest pair}}}{E(\nu)} = \frac{(E(\nu) - \lim_{s \to \nu+\varepsilon} E(s))}{E(\nu)} = \frac{1}{2(j-1)} \quad \text{for } \nu = \frac{j}{2j-1}. \quad (11)$$

It is noteworthy that both the energy $E(\nu)$ and the energy gap $E(\nu) - \lim_{s \to \nu+\varepsilon} E(s)$ are negative values. This mechanism is clarified in Section 3.

All the *nearest electron* (or *hole*) *pairs* are forbidden to transfer to any vacant (or filled) state at the filling factors of $\nu = (2j-1)/(2j)$ (or $\nu = 1/(2j)$). This mechanism is examined in Section 4.

At the filling factors of $\nu = 7/11$, $4/11$, $4/13$, $5/13$, $5/17$, and $6/17$, some of the *nearest electron* (or *hole*) *pairs* are allowed to transfer to all vacant (or filled) states. This case yields small energy gaps, for example,

$$\frac{\Delta E_{\text{nearest pair}}}{E(\nu)} = \frac{(E(\nu) - \lim_{s \to \nu+\varepsilon} E(s))}{E(\nu)} \approx \frac{0.006493}{0.103896} \quad \text{for } \nu = \frac{7}{11} \quad (12)$$

which is investigated in Section 5. Thus, the present theory produces a gap structure or a gapless structure for each fractional filling factor. The theoretical results are in a good agreement with the experimental data.

We examine another type of gap which indicates the excitation energy gap from the ground state to excited states. This new gap is highly correlated with the gap in the spectrum of energy versus filling factor. The mechanism is studied in Section 6.

2. Most Uniform Configuration of Electrons

We can find out the many-electron states with the minimum energy of H_D for any filling factor. As most easy examples, we show the case of $\nu = 1/3$ and $\nu = 2/3$. Figures 2(a) and 2(b) indicate the configurations of electrons with the minimum classical Coulomb energy at $\nu = 1/3$ and $2/3$, respectively.

Therein the bold line indicates a Landau state filled with electron, and the dashed line means an empty state. It is noteworthy that the current direction is described by the x-direction, and the Hall voltage direction is described by the y-direction (same as in Figure 1). Figure 2(a) shows the electron configuration with repeating of the arrangement (empty, filled, empty). This filling way is the most uniform configuration at $\nu = 1/3$ and then has the minimum classical Coulomb energy. The filling way in Figure 2(b) also has the minimum classical Coulomb energy at $\nu = 2/3$. It is easily seen that Figures 2(a) and 2(b) indicate the most uniform filling ways at $\nu = 1/3$ and $\nu = 2/3$, respectively.

We explain the searching method to find the electron configuration with the minimum Coulomb energy, because it is nontrivial to find the filling way for any fractional filling factor $\nu < 1$. In order to clarify the explanation, we consider one example of $\nu = 3/5$. We compare the classical Coulomb energies of the following two cases.

Case 1. In the whole region, three electrons exist inside every 5 sequential landau states. Then the filling factor becomes 3/5.

Case 2. Two electrons exist in 5 sequential Landau states for some parts, and four electrons exist in 5 sequential Landau states for some other parts. And the average filling factor is equal to 3/5.

The Coulomb energy of Case 1 is smaller than one of Case 2 because the filling way of Case 1 is more uniform than one of Case 2. Therefore, it is sufficient to consider all the

filling ways inside 5 sequential states. They are 10 filling ways as shown in Figure 3.

The five filling ways (a-1, a-2, a-3, a-4, and a-5) give the same electron configuration A by numerous repeating of themselves except both end parts. The electron configuration A is shown in Figure 4(a). The both end parts can be neglected for macroscopic number of electrons in a quantum Hall device.

Similarly the five filling ways (b-1, b-2, b-3, b-4, and b-5) in Figure 3 give the same electron configuration B as Figure 4(b). It is clear that the electron configuration A of Figure 4(a) has the classical Coulomb energy smaller than one of configuration B at $\nu = 3/5$.

It is noteworthy to examine the connections between different arrangements in Figure 3. We draw the connections of (a-1 and a-2), (a-1 and a-3), (a-1 and a-4), and (a-1 and a-5) in Figure 5 where the first filling way is red coloured, and the second filling way is blue coloured. All the connections include green areas where 2 electrons or 4 electrons exist inside five sequential Landau sates as in Figure 5.

Therefore, these connections belong to Case 2 and then have a classical Coulomb energy larger than one of configuration A in Figure 4(a).

For any filling factor $\nu = r/q$, r electrons should exist in q sequential Landau states everywhere. All filling ways have the number of $q!/(r!(q-r)!)$. We can draw all the filling ways and then find out the most uniform configuration of electrons. This procedure is applied to the cases with denominator $q = 2, 3, 4, 5, 6, 7, 8$. Then, we get the filling ways with the minimum classical Coulomb energy as drawn in Figure 6 (We abbreviate equivalent filling ways. For example only the filling way a-1 is drawn, and other filling ways a-2, a-3, a-4, a-5 are abbreviated for $\nu = 3/5$). These filling ways are called unit arrangements for each filling factors.

When we repeat the unit arrangement in Figure 6, we obtain the electron configuration with the minimum classical Coulomb energy at each filling factor.

We draw some examples with higher Coulomb energy for the denominator $q = 7, 8$ in Figure 7. Comparison of Figure 6 with Figure 7 reveals the fact that the unit arrangements in Figure 6 have more uniformity than ones in Figure 7.

Thus only one configuration has the minimum classical Coulomb energy among the enormous many configurations. The whole-electron configuration is created by repeating of only one unit arrangement of electron at any fractional number of ν.

3. Gap Structure in the Neighbourhood of $\nu = j/(2j \pm 1)$

3.1. Calculation of Binding Energy at $\nu = j/(2j-1)$. The shape of Landau wave function with $L = 0$ is schematically drawn by a straight line. We draw the most uniform electron configuration at $\nu = j/(2j-1)$ in Figure 8 where solid lines indicate the Landau orbitals filled with electron, and dashed lines indicate the vacant Landau orbitals. Therein, *nearest electron pairs* are red-coloured, and single electrons are blue-coloured. The Coulomb transitions from the nearest electron

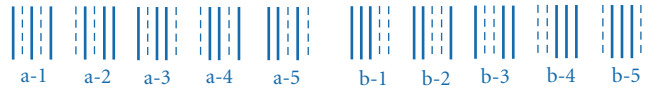

Figure 3: All unit arrangements of electron configurations for $\nu = 3/5$.

pair AB are illustrated by black arrows in Figure 8. The x and y directions are drawn in the upper left corner.

The electron configurations in Figure 8 have the minimum classical Coulomb energy for each filling factors. In order to explain the calculation of the second-order perturbation energy, we draw again the most uniform electron configuration of $\nu = 2/3$ in Figure 9. Therein the first transition is expressed by black arrows, and the second transition is expressed by green arrows and so on.

The momenta of the *nearest electron pair* AB are described by p_A, p_B, respectively. When electron A transfers to the first orbital to the left, the initial momentum p_A decreases by $2\pi\hbar/\ell$ according to (2). After the transition, the electron A has a new momentum p'_A as

$$p'_A = p_A - \frac{2\pi\hbar}{\ell}. \tag{13}$$

The other electron B transfers to the momentum p'_B. Then the total momentum conservation in the x-direction gives the following relation:

$$p'_A + p'_B = p_A + p_B. \tag{14}$$

Substitution of (13) into (14) yields the momentum p'_B as

$$p'_B = p_B + \frac{2\pi\hbar}{\ell}. \tag{15}$$

This momentum increment means that the electron B should transfer from its original orbital to the first orbital to the right because of (2) and (15). This transition is allowed because the right orbital is empty as in Figure 9.

Similarly the *nearest electron pair* AB can transfer to the other empty states, and the momenta after the transition are given by

$$\begin{aligned} p'_A &= p_A - \Delta p, \\ p'_B &= p_B + \Delta p, \end{aligned} \tag{16}$$

where the momentum transfer Δp at $\nu = 2/3$ has the values as

$$\Delta p = \frac{(3j+1)2\pi\hbar}{\ell} \quad \text{for } j = 0, \pm 1, \pm 2, \pm 3, \ldots \tag{17}$$

because the electrons are possible to transfer to empty orbitals only. (In this paper we investigate the case that all the electron spins have an opposite direction of magnetic field. Another case is discussed in the other articles [14–16]). The second-order perturbation energy of the *nearest electron pair* AB is given by

$$\begin{aligned} \varsigma_{\nu=2/3} &= \sum_{\Delta p=(3j+1)2\pi\hbar/\ell \text{ for } j=0,\pm1,\pm2,\ldots} \mathrm{R} \\ \mathrm{R} &= \frac{\langle p_A, p_B | H_I | p'_A, p'_B \rangle \langle p'_A, p'_B | H_I | p_A, p_B \rangle}{W_G - W_{\text{excite}}(p_A \to p'_A, p_B \to p'_B)}. \end{aligned} \tag{18}$$

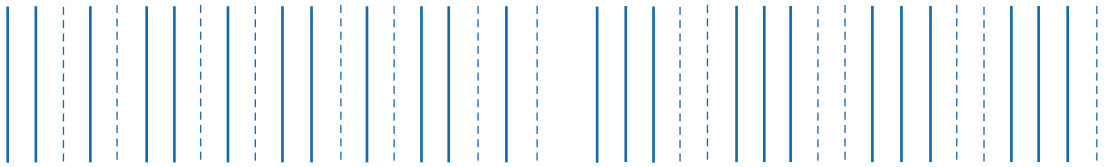

(a) (b)

Figure 4: (a) Configuration A at $\nu = 3/5$. (b) Configuration B at $\nu = 3/5$.

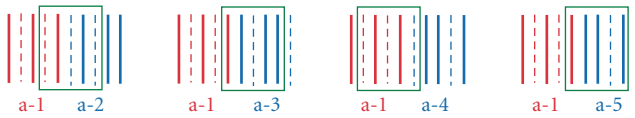

Figure 5: Connections between different arrangements.

We introduce the following summation Z as

$$Z = -\sum_{\Delta p \neq 0, -2\pi\hbar/\ell}^{\text{all}} \frac{\langle p_A, p_B | H_I | p'_A, p'_B \rangle \langle p'_A, p'_B | H_I | p_A, p_B \rangle}{W_G - W_{\text{excite}}(p_A \to p'_A, p_B \to p'_B)}, \tag{19}$$

where the momentum transfer Δp takes all values $(2\pi\hbar/\ell) \times$ integer except $\Delta p = 0$ and $\Delta p = -2\pi\hbar/\ell$. The transferred states with $\Delta p = 0$ and $\Delta p = -2\pi\hbar/\ell$ are the same state as the initial state. This state is eliminated in the summation of (19) because the diagonal matrix element of H_I is zero. Therefore, the denominator is not zero and has a negative value. The definition of Z includes (-1) in the right-hand side, and the denominator is a negative value. Accordingly the value of Z is positive.

We can systematically describe the perturbation energies at any filling factors by using the value of Z. We compare Z with the perturbation energy $\varsigma_{\nu=2/3}$ of (18). The interval of the momentum transfer is $3 \times 2\pi\hbar/\ell$ in the summation $\varsigma_{\nu=2/3}$. On the other hand, the summation Z is performed by the momentum interval $2\pi\hbar/\ell$. The interval value is very small for a quantum Hall device with a macroscopic size and then we get

$$\varsigma_{\nu=2/3} = -\frac{1}{3}Z. \tag{20}$$

Thus, we can express the perturbation energy $\varsigma_{\nu=2/3}$ of the *nearest electron pair* by the summation Z. The perturbation energies depend upon ℓ and B, namely, device size and magnetic field strength. These dependences are included in the summation Z.

The number of *nearest electron pairs* is $(1/2)N$ at $\nu = 2/3$, where N is the total number of electrons. Accordingly the total perturbation energy $E_{\text{nearest pair}}$ of all *nearest electron pairs* is obtained as

$$E_{\text{nearest pair}} = \frac{1}{2}N \times \varsigma_{\nu=2/3} = -\frac{1}{6}ZN, \quad \text{for } \nu = \frac{2}{3}. \tag{21}$$

Similar calculation leads the second order perturbation energy of *nearest electron pairs* at any filling factor of $\nu = j/(2j-1)$ as follows [16].

Therein, j electrons partially occupy each sequential $(2j-1)$ Landau states, and then $(j-1)$ Landau states are empty for each sequential $(2j-1)$ Landau states. Any *nearest electron pair* can transfer to all the empty states as in Figure 8. The number of transitions is equal to $(j-1)$ for each $(2j-1)$ Landau states. Therefore, the second-order perturbation energy per pair is given by

$$\varsigma_{\nu=j/(2j-1)} = -\frac{j-1}{2j-1}Z, \quad \text{for } \nu = \frac{j}{(2j-1)}. \tag{22}$$

The number of *nearest electron pairs* is $(1/j)N$ at $\nu = j/(2j-1)$, where N is the total number of electrons. Accordingly the total perturbation energy $E_{\text{nearest pair}}$ from all *nearest electron pairs* is obtained as

$$\begin{aligned} E_{\text{nearest pair}} &= \frac{N}{j}\varsigma_{\nu=j/(2j-1)} \\ &= -\frac{j-1}{j(2j-1)}ZN, \quad \text{for } \nu = \frac{j}{(2j-1)}. \end{aligned} \tag{23}$$

The *nearest electron pair* energy per electron is given by

$$\chi\left(\nu = \frac{j}{2j-1}\right) = -\frac{(j-1)Z}{(j(2j-1))}, \quad \text{for } \nu = \frac{j}{(2j-1)}. \tag{24}$$

3.2. Gap Structure at $\nu = j/(2j-1)$. It has been clarified in the previous subsection that all the nearest electron pairs can transfer to all empty Landau orbitals at the filling factor of $\nu = j/(2j-1)$. We next examine the perturbation energies in the neighbourhood of $\nu = j/(2j-1)$. The fraction $\nu = (j(2s)-1)/((2j-1)(2s)-2)$ approaches $\nu = j/(2j-1)$ in the limit of infinitely large s. In the case of $j = 4, s = 2$, the fraction is equal to

$$\nu = \frac{(j(2s)-1)}{((2j-1)(2s)-2)} = \frac{15}{26}. \tag{25}$$

The most uniform electron configuration is illustrated in Figure 10.

It is noteworthy that some nearest electron pairs cannot transfer to some empty states because of momentum conservation and Pauli's exclusion principle. We take this prohibition of the transitions into consideration and obtain the perturbation energy of nearest electron pairs as follows:

$$\begin{aligned} E_{\text{nearest pair}} &= \left[-2 \times \left(\frac{8}{26}\right)Z - 2 \times \left(\frac{10}{26}\right)Z\right] \\ &\quad \times \left(\frac{1}{15}\right)N = -\frac{36}{26 \times 15}ZN, \quad \text{for } \nu = \frac{15}{26}. \end{aligned} \tag{26}$$

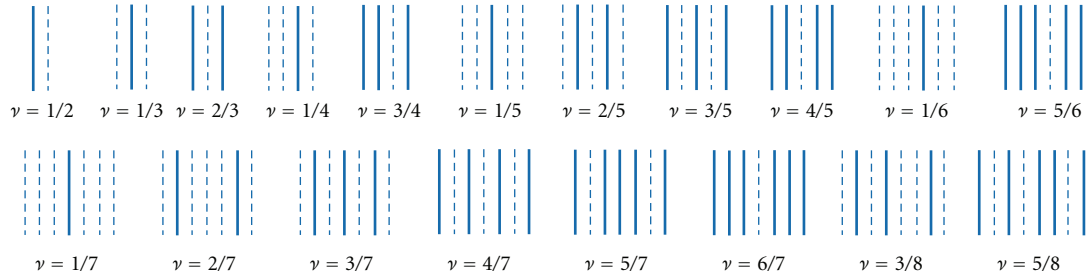

Figure 6: Most uniform unit arrangements of electron configuration.

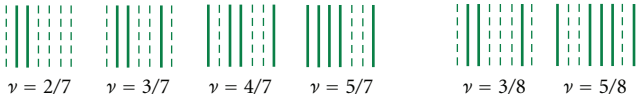

Figure 7: Filling ways with higher classical Coulomb energy.

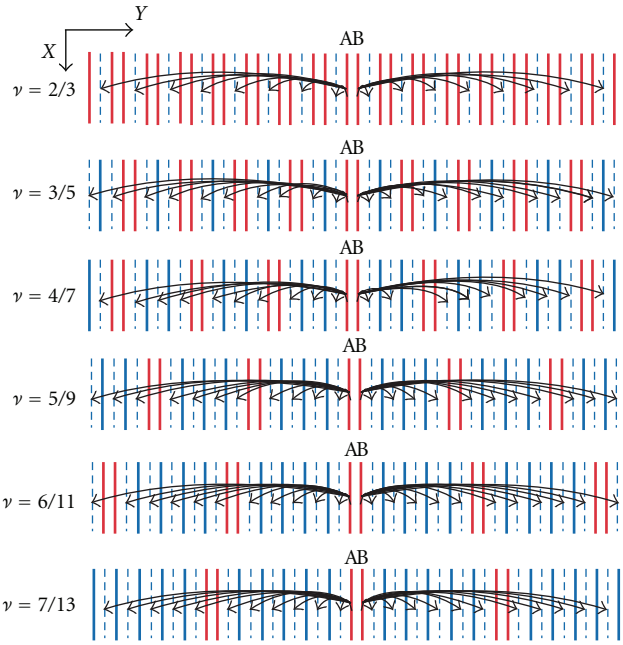

Figure 8: Allowed transitions of *nearest electron pair* at $\nu = j/(2j-1)$.

This calculation process can be extended to any integer s as follows:

$$E_{\text{nearest pair}} = \left[-2\times\left(\frac{(4s)}{(14s-2)}\right)Z-2\times\left(\frac{(4s+2)}{(14s-2)}\right)Z\cdots \cdots-2\times\left(\frac{(6s-2)}{(14s-2)}\right)Z\right] \times\frac{N}{(8s-1)}. \tag{27}$$

The result indicates the perturbation energy of nearest electron pairs in the neighbourhood of $\nu = 4/7$.

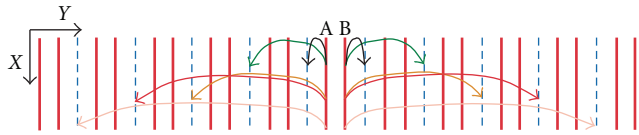

Figure 9: Coulomb transitions from nearest electron pair AB at $\nu = 2/3$. (The electric current flows along the x-direction. The momentum value is related to its central position of the y direction as in (2)).

Next we examine the neighbourhood of $\nu = j/(2j-1)$ for any integer of j. That is to say we consider the filling factor of $\nu = (j(2s)-1)/((2j-1)(2s)-2)$. We introduce new three parameters as follows:

$$\alpha = ((2j-1)(2s)-2), \qquad \beta = (j(2s)-1), \qquad \gamma = ((j-1)(2s)-1). \tag{28}$$

The parameter α is the number of orbitals in unit arrangement, β is the number of electrons in unit arrangement, and γ is the number of empty orbitals in unit arrangement. Accordingly we replace $(8s-1)$ into β and also replace $(14s-2)$ into α in (27). Then we get

$$E_{\text{nearest pair}} = \left[-2\times\left(\frac{(4s)}{\alpha}\right)Z-2 \times\left(\frac{(4s+2)}{\alpha}\right)Z\cdots-2\times\left(\frac{(6s-2)}{\alpha}\right)Z\right]\times\frac{N}{\beta}, \tag{29}$$

where $(6s-2)$ indicate $\gamma-1$. Accordingly $(4s)$ is replaced to $\gamma+1-2s$, and then we obtain that

$$\begin{aligned} E_{\text{nearest pair}} &= \left[-2\times\left(\frac{(\gamma+1-2s)}{\alpha}\right)Z-2 \times\left(\frac{(4s+2)}{\alpha}\right)\times Z\cdots-2\times\left(\frac{(\gamma-1)}{\alpha}\right)Z\right]\times\frac{N}{\beta}, \\ E_{\text{nearest pair}} &= [-2\times(\gamma+1-2s)-2 \times(\gamma+3-2s)\cdots-2\times(\gamma-1)]\frac{Z}{\alpha}\times\frac{N}{\beta}, \\ E_{\text{nearest pair}} &= [-(2\gamma-2s)s]\frac{Z}{\alpha}\times\frac{N}{\beta} \quad \text{at } \nu=\frac{\beta}{\alpha}. \end{aligned} \tag{30}$$

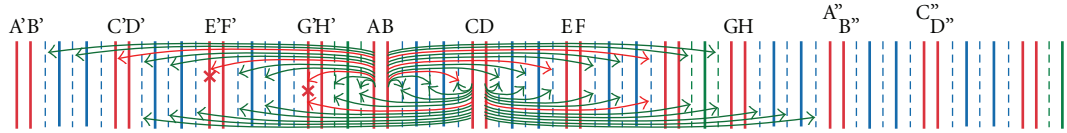

Figure 10: Transitions from nearest electron pairs for $\nu = 15/26$.

Substitution of (28) into (30) yields

$$E_{\text{nearest pair}} = -\frac{((2j-3)2s-2)s}{((2j-1)(2s)-2)}\frac{ZN}{(j(2s)-1)} \quad \text{at } \nu = \frac{(j(2s)-1)}{((2j-1)(2s)-2)}. \tag{31}$$

Thus, we have obtained the perturbation energy of the nearest electron pairs for any integers of j and s. Equation (31) gives the limiting value from the right for $s \to \infty$ because $\nu = \beta/\alpha$ is larger than $j/(2j-1)$. We have

$$\nu = \frac{\beta}{\alpha} = \frac{(j(2s)-1)}{((2j-1)(2s)-2)} \xrightarrow[s\to\infty]{} \frac{j}{(2j-1)}, \tag{32a}$$

$$E_{\text{nearest pair}} = -\frac{((2j-3)2s-2)s}{((2j-1)(2s)-2)}\frac{ZN}{(j(2s)-1)} \xrightarrow[s\to\infty]{} -\frac{(2j-3)ZN}{2j(2j-1)} \quad \text{at } \nu = \frac{j}{2j-1}+\varepsilon, \tag{32b}$$

where ε indicates an infinitesimally small positive value. Equation (23) indicates the perturbation energy of nearest electron pairs at $\nu = j/(2j-1)$ as

$$E_{\text{nearest pair}} = -\frac{(j-1)ZN}{j(2j-1)} \quad \text{at } \nu = \frac{j}{2j-1}, \tag{33}$$

$$\chi\left(\frac{j}{2j-1}\right) = \frac{E_{\text{nearest pair}}}{N} = -\frac{(j-1)Z}{(j(2j-1))}. \tag{34}$$

Equation (32b) means the limiting value of *nearest pair* perturbation energy from the right at $\nu = j/(2j-1)$. The perturbation energy (33) at $\nu = j/(2j-1)$ is lower than the limiting value (32b), and, therefore, the energy gap is equal to

$$\Delta E_{\text{nearest pair}} = E(\nu) - \lim_{s\to\nu+\varepsilon} E(s) = -\frac{ZN}{2j(2j-1)} \quad \text{for } \nu = \frac{j}{2j-1}. \tag{35}$$

Next we calculate the limiting value from the left. We consider the fraction $\nu = (j(2s)+1)/((2j-1)(2s)+2)$ which is smaller than $\nu = j/(2j-1)$. New three parameters α', β', and γ' are defined as

$$\alpha' = ((2j-1)(2s)+2), \qquad \beta' = (j(2s)+1), \qquad \gamma' = ((j-1)(2s)+1). \tag{36}$$

The parameter α' is the number of orbitals in unit arrangement, β' is the number of electrons in unit arrangement, and γ' is the number of empty orbitals in unit arrangement. The filling factor is given by $\nu = \beta'/\alpha'$ as

$$\nu = \frac{\beta'}{\alpha'} = \frac{(j(2s)+1)}{((2j-1)(2s)+2)}. \tag{37}$$

The total transition energy from all the *nearest electron pairs* is equal to

$$E_{\text{nearest pair}} = [-(2\gamma' - 2s)s]\frac{Z}{\alpha'} \times \frac{N}{\beta'} \quad \text{at } \nu = \frac{\beta'}{\alpha'}. \tag{38}$$

Limiting values of (37) and (38) are

$$\nu = \frac{(j(2s)+1)}{((2j-1)(2s)+2)} \xrightarrow[s\to\infty]{} \frac{j}{(2j-1)}, \qquad E_{\text{nearest pair}} = -\frac{((2j-3)2s+2)s}{((2j-1)(2s)+2)}\frac{ZN}{(j(2s)+1)} \xrightarrow[s\to\infty]{} -\frac{(2j-3)ZN}{2j(2j-1)} \quad \text{at } \nu = \frac{j}{2j-1}-\varepsilon. \tag{39}$$

This limiting value from the left is compared with the original value at $\nu = j/(2j-1)$, and then the original value is lower than the limiting value from the left as

$$\Delta E_{\text{nearest pair}} = E(\nu) - \lim_{s\to\nu-\varepsilon} E(s) = -\frac{ZN}{2j(2j-1)} \quad \text{for } \nu = \frac{j}{2j-1}. \tag{40}$$

Equations (35) and (40) indicate that the limiting values from both sides of $\nu = j/(2j-1)$ are higher than the original value at $\nu = j/(2j-1)$.

The gap structure is produced from the property that all the *nearest electron pairs* are possible to transfer to all empty states at $\nu = j/(2j-1)$. When the filling factor ν changes from $j/(2j-1)$ by an infinitesimally small value, some of the transitions are forbidden. That is to say the number of allowed transitions decreases drastically. This property is caused by the most uniform electron configuration, Fermi-Dirac statistics, and momentum conservation. The drastic change also appears in higher order of the perturbation energy. The higher-order perturbations are studied in the other article.

Table 1 shows the discontinuous structure of the perturbation energies at the filling factors of $\nu = j/(2j-1)$, where ε expresses an infinitesimally small positive value. Therefore, $+\varepsilon$ indicates the limiting process from the right, and $-\varepsilon$ indicates the limiting process from the left.

Table 1: Energy gaps of *nearest electron pairs* per electron at $\nu = j/(2j-1)$.

ν	$E_{\text{nearest pair}}/N$	ν	$\lim(E_{\text{nearest pair}}/N)$	$\Delta\varepsilon_+(\nu) = \Delta\varepsilon_-(\nu)$
2/3	$-(1/6)Z$	$(2/3) \pm \varepsilon$	$-(1/12)Z$	$-(1/12)Z$
3/5	$-(2/15)Z$	$(3/5) \pm \varepsilon$	$-(3/30)Z$	$-(1/30)Z$
4/7	$-(3/28)Z$	$(4/7) \pm \varepsilon$	$-(5/56)Z$	$-(1/56)Z$
5/9	$-(4/45)Z$	$(5/9) \pm \varepsilon$	$-(7/90)Z$	$-(1/90)Z$
6/11	$-(5/66)Z$	$(6/11) \pm \varepsilon$	$-(9/132)Z$	$-(1/132)Z$
7/13	$-(6/91)Z$	$(7/13) \pm \varepsilon$	$-(11/182)Z$	$-(1/182)Z$
8/15	$-(7/120)Z$	$(8/15) \pm \varepsilon$	$-(13/240)Z$	$-(1/240)Z$

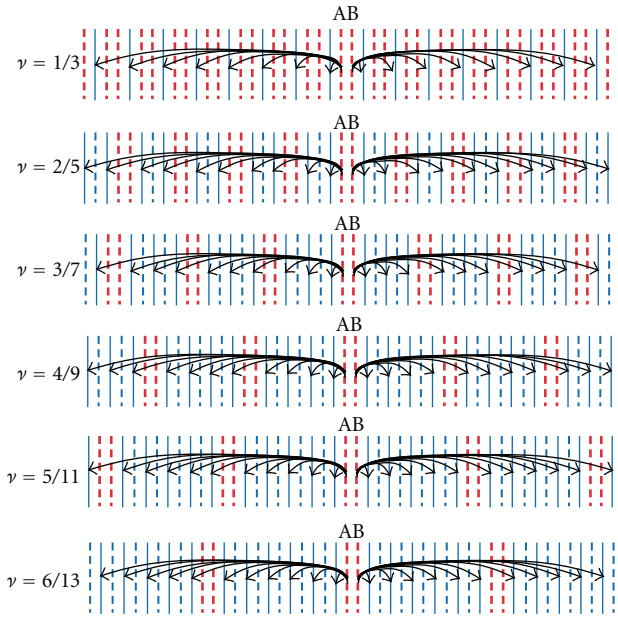

Figure 11: Coulomb transitions from nearest hole pair AB.

3.3. Gap Structure at $\nu = j/(2j+1)$. We draw the most uniform electron configuration at $\nu = j/(2j+1)$ in Figure 11.

Therein, solid lines indicate the Landau orbitals filled with electron, and dashed lines indicate the vacant Landau orbitals. *Nearest hole pairs* are red coloured, and single holes are blue coloured. The Coulomb transitions from the *nearest hole pair* AB are drawn by black arrows in Figure 11. Using the same method as in the previous section, we can estimate the perturbation energies of the *nearest hole pairs* $E_{\text{nearest hole pair}}$. The result is as follows:

$$E_{\text{nearest hole pair}} = -\frac{j}{(j+1)(2j+1)} Z_H N_H \quad \text{at } \nu = \frac{j}{2j+1}, \tag{41}$$

where N_H is the total number of holes. We obtain the pair energy per hole as

$$\frac{E_{\text{nearest hole pair}}}{N_H} = -\frac{j}{(j+1)(2j+1)} Z_H \quad \text{at } \nu = \frac{j}{2j+1}. \tag{42}$$

The energy per electron is

$$\frac{E_{\text{nearest hole pair}}}{N} = -\frac{1}{(2j+1)} Z_H \quad \text{at } \nu = \frac{j}{2j+1}. \tag{43}$$

We also calculate the perturbation energies in the neighbourhood of $\nu = j/(2j+1)$, and the results are

$$E_{\text{nearest hole pair}} = -\frac{((2j-1)2s-2)s}{((2j+1)(2s)-2)} \frac{Z_H N_H}{((j+1)(2s)-1)} \quad \text{at } \nu = \frac{((j)(2s)-1)}{((2j+1)(2s)-2)},$$
$$E_{\text{nearest hole pair}} = -\frac{((2j-1)2s+2)s}{((2j+1)(2s)+2)} \frac{Z_H N_H}{((j+1)(2s)+1)} \quad \text{at } \nu = \frac{((j)(2s)+1)}{((2j+1)(2s)+2)}. \tag{44}$$

The limiting values are obtained as

$$\frac{E_{\text{nearest hole pair}}}{N} \xrightarrow[s\to\infty]{} -\frac{2j-1}{2j(2j+1)} Z_H \quad \text{for } \nu = \frac{j}{2j+1} \pm \varepsilon. \tag{45}$$

We summarize the energy gaps of the *nearest hole pairs* at $\nu = j/(2j+1)$ in Table 2. The rightmost column means the energy gap per electron (not per hole).

Tables 1 and 2 show the gap structure of the fractional filling states at $\nu = j/(2j \pm 1)$ because the perturbation energy is lower than one of each neighbourhood.

3.4. Comparison between Experimental Data and Nearest Pair Energy at $\nu = j/(2j \pm 1)$. Many electrons in the electric current are scattered by impurities and thermal vibrations. These scatterings yield the diagonal resistance of the x direction.

At $\nu = j/(2j \pm 1)$, we have theoretically estimated the energy gaps in the spectrum of energy versus filling factor in Sections 3.2 and 3.3. The energy gaps in the spectrum produce the plateaus in Hall resistance curve (confinements of Hall resistance). The excitation-energy gap from the ground state is highly correlated with the energy gap in the spectrum as discussed in Section 6.

The excitation-energy gaps suppress the electron scatterings. Then the diagonal resistance becomes small. This

Table 2: Energy gaps of *nearest hole pairs* per electron at $\nu = j/(2j+1)$.

ν	$E_{\text{nearest pair}}/N_H$	$E_{\text{nearest pair}}/N$	ν	$\lim(E_{\text{nearest pair}}/N)$	$\Delta\varepsilon_+(\nu) = \Delta\varepsilon_-(\nu)$
1/3	$-(1/6)Z_H$	$-(1/3)Z_H$	$(1/3) \pm \varepsilon$	$-(1/6)Z_H$	$-(1/6)Z_H$
2/5	$-(2/15)Z_H$	$-(1/5)Z_H$	$(2/5) \pm \varepsilon$	$-(3/20)Z_H$	$-(1/20)Z_H$
3/7	$-(3/28)Z_H$	$-(1/7)Z_H$	$(3/7) \pm \varepsilon$	$-(5/42)Z_H$	$-(1/42)Z_H$
4/9	$-(4/45)Z_H$	$-(1/9)Z_H$	$(4/9) \pm \varepsilon$	$-(7/72)Z_H$	$-(1/72)Z_H$
5/11	$-(5/66)Z_H$	$-(1/11)Z_H$	$(5/11) \pm \varepsilon$	$-(9/110)Z_H$	$-(1/110)Z_H$
6/13	$-(6/91)Z_H$	$-(1/13)Z_H$	$(6/13) \pm \varepsilon$	$-(11/156)Z_H$	$-(1/156)Z_H$
7/15	$-(7/120)Z_H$	$-(1/15)Z_H$	$(7/15) \pm \varepsilon$	$-(13/210)Z_H$	$-(1/210)Z_H$

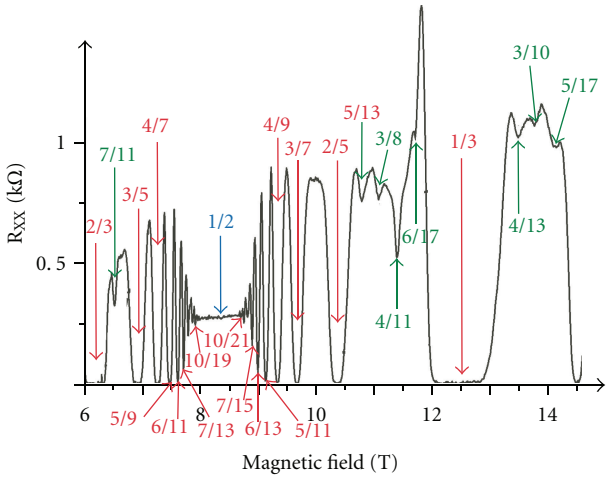

Figure 12: Many local minima of the diagonal resistance in the region of $2/3 \geq \nu \geq 1/3$. This experimental result has been obtained in [2].

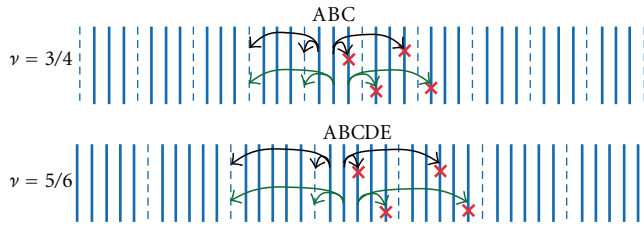

Figure 13: All Coulomb transitions from nearest electron pairs are forbidden.

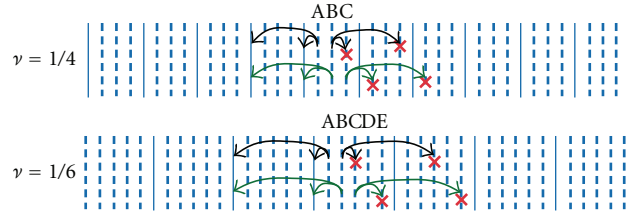

Figure 14: All Coulomb transitions from nearest hole pairs are forbidden.

mechanism produces local minima in the diagonal resistance curve. The theoretical results in Tables 1 and 2 are in a good accordance with the experimental data of Figure 12.

The local minima appear at the filling factors of ν =2/3, 3/5, 4/7, 5/9, 6/11, 7/13, 8/15,... and ν = 7/15, 6/13, 5/11, 4/9, 3/7, 2/5, 1/3 which are indicated by red colour in Figure 12. Furthermore, there are small local minima in the curve of diagonal resistance versus magnetic field strength. The fractions are 7/11, 5/13, 3/8, 4/11, 6/17, 4/13, 3/10, and 5/17 which are coloured by green in Figure 12. We will examine the FQH states with $\nu = 7/11, 4/11, 4/13, 5/13, 5/17, 6/17$ in the later Section 5. The remaining FQH states with $\nu = 3/8, 5/8, 3/10$ have even denominators and have been already investigated in [17].

4. Gapless Structure of Nearest Pair Energy at $\nu = 1/(2j)$ and $\nu = (2j-1)/(2j)$

The most uniform electron configurations are illustrated in Figure 13 at $\nu = (2j-1)/(2j)$. The filling factors have even number of the denominator. As an example, we examine the case of $\nu = 3/4$. When electron A transfers to the fifth orbital to the left, electron B should transfer to the fifth orbital to the right. However, the fifth orbital is already filled with electron. Therefore, this transition is forbidden. Similarly all the nearest electron pairs cannot transfer to empty states at $\nu = (2j-1)/(2j)$.

Next we draw the most uniform electron configuration for $\nu = 1/(2j)$ in Figure 14. The hole pairs AB and BC cannot transfer to any filled orbitals at $\nu = 1/4$ as in Figure 14. All the nearest hole pairs cannot transfer to any filled orbitals at $\nu = 1/(2j)$ for any integer of j. Therefore, the perturbation energies of the nearest electron (or hole) pairs are zero for all order perturbations at $\nu = (2j-1)/(2j)$ (or $\nu = 1/(2j)$).

That is to say we obtain the following relations:

$$\frac{E_{\text{nearest electron pair}}}{N} = 0, \quad \text{for } \nu = \frac{(2j-1)}{(2j)}, \qquad \frac{E_{\text{nearest hole pair}}}{N_H} = 0, \quad \text{for } \nu = \frac{1}{(2j)}. \tag{46}$$

We show the perturbation energies of *nearest electron pairs* and *nearest hole pairs* in Table 3.

Consequently the states with $\nu = (2j-1)/(2j)$ (and $\nu = 1/(2j)$) are not confined in the Hall resistance curve [18–23].

Table 3: *Nearest pair* energies at $\nu = (2j-1)/(2j)$ and $\nu = 1/(2j)$.

ν	$E_{\text{nearest pair}}/N$	ν	$E_{\text{nearest pair}}/N_H$
1/2	0		
3/4	0	1/4	0
5/6	0	1/6	0
7/8	0	1/8	0

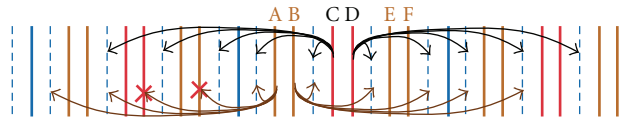

Figure 15: Coulomb transitions of nearest electron pairs at $\nu = 7/11$.

5. Special States with Several Fractional Filling Factors

In this section we examine the states with the filling factors $\nu = 7/11, 4/11, 4/13, 5/13, 5/17$, and $6/17$. The most uniform electron configuration with $\nu = 7/11$ is schematically drawn in Figure 15. There are three pairs of nearest electrons in every unit arrangement, namely, (filled, empty, filled, filled, empty, filled, filled, empty, filled, filled, empty). The orbitals filled with electron are illustrated by solid lines, and the empty orbitals are illustrated by dashed lines.

The *nearest electron pair* CD can transfer to all empty orbitals. Then the perturbation energy of the pair CD is equal to

$$\varsigma_{\text{CD}} = -\left(\frac{4}{11}\right)Z. \tag{47}$$

The *nearest electron pairs* AB and EF transfer to two empty states per unit arrangement and have the perturbation energies ς_{AB} and ς_{EF} as

$$\varsigma_{\text{AB}} = \varsigma_{\text{EF}} = -\left(\frac{2}{11}\right)Z, \tag{48}$$

$$\begin{aligned}\left(E_{\text{nearest pair}}\right)_{\nu=7/11} &= \left(-\frac{4}{11}Z - \frac{2}{11}Z - \frac{2}{11}Z\right)\frac{1}{7}N, \\ &= -\frac{8}{77}ZN, \quad \text{for } \nu = \frac{7}{11},\end{aligned} \tag{49}$$

$$\left(\frac{E_{\text{nearest pair}}}{N}\right)_{\nu=7/11} = -\frac{8}{77}Z \approx -0.103896\times Z, \quad \text{for } \nu = \frac{7}{11}. \tag{50}$$

We examine the neighbourhood of $\nu = 7/11$ which are $\nu = (7s-2)/(11s-3)$ and $\nu = (7s+2)/(11s+3)$. The most uniform electron configuration at $\nu = (7s \pm 2)/(11s \pm 3)$ is systematically produced by modulation of the configuration as Figure 15. Then the perturbation energy of the nearest

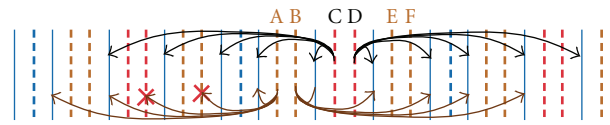

Figure 16: Coulomb transitions of nearest hole pairs at $\nu = 4/11$.

electron pairs is calculated by the use of the computer program. The calculation results for $s = 100$ are

$$\begin{aligned}&\left(\frac{E_{\text{nearest pair}}}{N}\right)_{\nu=698/1097} \\ &\quad = -\frac{74601}{765706}Z = -0.0974277\times Z, \quad \text{for } \nu_- = \frac{698}{1097}, \\ &\left(\frac{E_{\text{nearest pair}}}{N}\right)_{\nu=702/1103} \\ &\quad = -\frac{75401}{774306}Z = -0.0973788\times Z, \quad \text{for } \nu_+ = \frac{702}{1103}.\end{aligned} \tag{51}$$

We also calculate the case of $s = 1000$ the results of which are

$$\begin{aligned}&\left(\frac{E_{\text{nearest pair}}}{N}\right) \\ &\quad = -\frac{7496001}{76957006}Z = -0.097405\times Z, \quad \text{for } \nu_- = \frac{6998}{10997}, \\ &\left(\frac{E_{\text{nearest pair}}}{N}\right) \\ &\quad = -\frac{7504001}{77043006}Z = -0.0974002\times Z, \quad \text{for } \nu_+ = \frac{7002}{11003}.\end{aligned} \tag{52}$$

We compare the case of $s = 100$ with $s = 1000$ and find that the energies (51)–(52) are nearly equal to each other. Then the limiting values from both sides are approximately equal to

$$\lim_{\nu\to(7/11)\pm\varepsilon}\left(\frac{E_{\text{nearest pair}}}{N}\right) \approx -0.097403\times Z, \quad \text{for } \nu_\pm = \frac{7}{11}\pm\varepsilon. \tag{53}$$

The perturbation energy per electron is $(-0.103896\times Z)$ at $\nu = 7/11$, and therefore the energy gap appears at $\nu = 7/11$ as in (50) and (53)

$$\left(\frac{E_{\text{nearest pair}}}{N}\right)_{\nu=7/11} - \lim_{\nu\to(7/11)\pm\varepsilon}\left(\frac{E_{\text{nearest pair}}}{N}\right) \approx -0.006493\times Z. \tag{54}$$

Next we examine the case of $\nu = 4/11$. We schematically draw the most uniform electron configuration of $\nu = 4/11$ in Figure 16.

Then the perturbation energy of the nearest hole pairs is obtained as

$$\begin{aligned}&\left(E_{\text{nearest pair}}\right)_{\nu=4/11} = -\frac{8}{77}Z_H N_H, \quad \text{for } \nu = \frac{4}{11}, \\ &\left(\frac{E_{\text{nearest pair}}}{N_H}\right)_{\nu=4/11} = -\frac{8}{77}Z_H, \quad \text{for } \nu = \frac{4}{11}, \\ &\left(\frac{E_{\text{nearest pair}}}{N}\right)_{\nu=4/11} = -\frac{8}{11\ \times\ 4}Z_H = -\frac{2}{11}Z_H, \quad \text{for } \nu = \frac{4}{11}.\end{aligned} \tag{55}$$

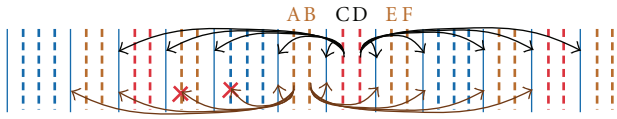

Figure 17: Coulomb transitions of nearest hole pair at $\nu = 4/13$.

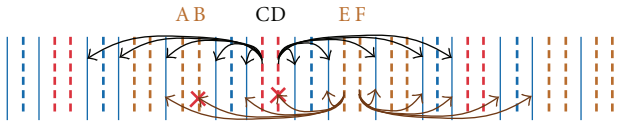

Figure 18: Coulomb transitions of nearest hole pair at $\nu = 5/13$.

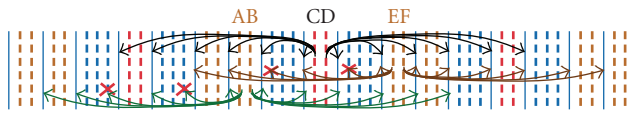

Figure 19: Coulomb transitions of nearest hole pair at $\nu = 5/17$.

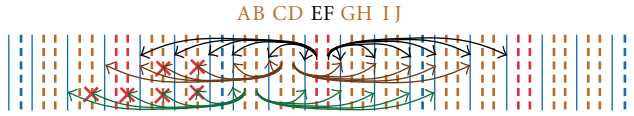

Figure 20: Coulomb transitions of nearest hole pair at $\nu = 6/17$.

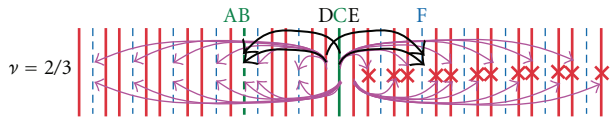

Figure 21: Electron configuration in excited state #1 at $\nu = 2/3$.

If the configuration continues infinitely (it is a good approximation for macroscopic size of a device), then Figure 16 has the left-right symmetry for the centre of the hole pair CD. These pairs like CD are coloured red. All the red pairs can transfer to all the electron states. On the other hand, there is no left-right symmetry for the centre of the pair AB or EF. The pairs are coloured brown. They cannot transfer to some electron states because of momentum conservation. The perturbation energy of the nearest hole pairs has the energy gap at $\nu = 4/11$ as in the case of $\nu = 7/11$.

Similar configurations are schematically drawn in Figures 17, 18, 19 and 20 for $\nu = 4/13, 5/13, 5/17, 6/17$.

All the red hole pairs can transfer to all electron states as in Figures 15–20. This property is violated by infinitesimally small changing of the value ν. When the value of ν varies from the original values $\nu = 4/13, 5/13, 5/17$, and $6/17$, the number of allowed transitions becomes small. Therefore, these states with $\nu = 4/13, 5/13, 5/17, 6/17$ are stable. This property is in accordance with the experimental data as it is shown by green colour in Figure 12. (The fractions $\nu = 3/8, 58, 3/10$ have been studied in [17].)

6. Excitation Energy of FQHS

We have used the term "energy gap" for the gap in the spectrum of energy versus filling factor in the previous sections. This gap produces the plateau in the Hall resistance curve [18–23]. There is another gap which indicates the minimum value of all excitation energies from the ground state to excited states with the same filling factor ν. We call it "excitation-energy-gap." We examine the excitation-energy gap for three filling factors in this section.

We first consider one of excited states at $\nu = 2/3$ which is illustrated in Figure 21. The electron configuration is created by the excitation from the ground state as follows: one electron in the orbital B transfers to the orbital C. This excitation from the ground state is shown by green color in Figure 21. The electron configuration expresses one of eigen states for the Hamiltonian H_D. This excited state #1 has new nearest-electron pairs CE and DC which have the perturbation energies via residual Coulomb transitions. As in Figure 21, no transition is allowed from the pair CE, and only two transitions are allowed from the pair DC. Forbidden transitions are drawn by pink color, and allowed transitions are drawn by black color.

The perturbation energies of the pairs CE and DC are described by the symbols ς'_{CE} and ς'_{DC}, respectively. The symbol ς' (symbol prime) means the perturbation energy for the excited state #1. The second-order perturbation energy ς'_{DC} is obtained as

$$\varsigma'_{DC} = \sum_{\Delta p=6(2\pi\hbar/\ell),-7(2\pi\hbar/\ell)} \frac{\langle p_D, p_C|H_I|p'_D, p'_C\rangle\langle p'_D, p'_C|H_I|p_D, p_C\rangle}{W_{state\#1} - W_{excite}(p_D \to p'_D, p_C \to p'_C)}. \tag{56}$$

We introduce the following summation Z' as:

$$Z' = -\sum_{\Delta p \neq 0,-2\pi\hbar/\ell}^{all} \frac{\langle p_D, p_C\,|\,H_I\,|\,p'_D, p'_C\rangle\,\langle p'_D, p'_C\,|\,H_I\,|\,p_D, p_C\rangle}{W_{state\#1} - W_{excite}(p_D \to p'_D, p_C \to p'_C)}. \tag{57}$$

This definition is similar to (19). We count the number of effective transitions which have the overlapping region between the initial Landau wave function and the final wave function. If the momentum transfer becomes lager than some critical value, then the transition matrix element becomes negligibly small.

The spreading width of Landau state is denoted by Δy, the value of which is about 10.5 nm for the case of $B \approx 6$[T]

$$\hbar \approx 1.0546 \times 10^{-34}\,\text{J s}, \quad e \approx 1.6022 \times 10^{-19}\,\text{C}, \quad \Delta y \approx 10.5\ [\text{nm}], \quad \text{for } B \approx 6\ [T]. \tag{58}$$

The interval width between nearest Landau orbitals is estimated as

$$\Delta\alpha = \frac{2\pi\hbar}{eB\ell} \approx 6.5 \times 10^{-4}\ [\text{nm}], \quad \text{for } \ell = 1\ [\text{mm}] = 10^6\ [\text{nm}], \tag{59}$$

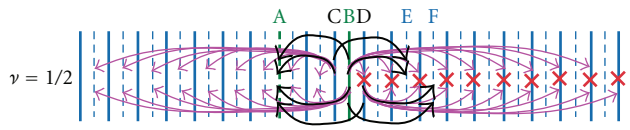

Figure 22: Electron configuration in excited state #2 at $\nu = 1/2$.

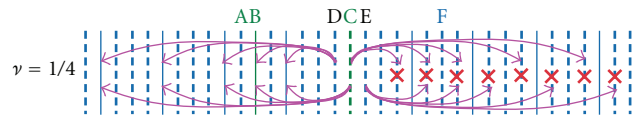

Figure 23: Electron configuration in excited state #3 at $\nu = 1/4$.

where we have applied $\ell = 1$ [mm] for the length of quantum Hall device. Then there are enormous many single-electron states inside the spreading width Δy. The number is

$$\frac{\Delta y}{\Delta \alpha} \approx \frac{\ell}{2\pi}\sqrt{\frac{eB}{\hbar}} \approx 2 \times 10^4. \tag{60}$$

Accordingly the effective momentum transfers satisfy the following relation:

$$|p'_{\mathrm{C}} - p_{\mathrm{C}}| \leq \frac{2\pi\hbar}{\ell} \times 2 \times 10^4. \tag{61}$$

Only two transitions are allowed from the pair DC, and therefore the ratio $-\varsigma'_{\mathrm{DC}}/Z'$ is about 10^{-4} as follows:

$$\frac{-\varsigma'_{\mathrm{DC}}}{Z'} \approx \frac{2}{(2 \times 10^4)} = 10^{-4}, \quad \text{for } \ell = 1 \text{ [mm]}. \tag{62}$$

Because this value is negligibly small, we can use the following approximation:

$$\varsigma'_{\mathrm{DC}} \approx -10^{-4} \times Z' \approx 0. \tag{63}$$

All the transitions from the pair CE are forbidden, and then the perturbation energy of the nearest pair CE is zero

$$\varsigma'_{\mathrm{CE}} = 0. \tag{64}$$

Furthermore, the nearest pair AB disappears by the excitation in Figure 21, and therefore the excitation-energy $\Delta E_{\text{excitation \#1}}$ is given by

$$\Delta E_{\text{excitation \#1}} = \varsigma'_{\mathrm{DC}} + \varsigma'_{\mathrm{CE}} - \varsigma_{\mathrm{AB}}, \tag{65}$$

where ς_{AB} indicates the summation (18) the result of which is equal to (20)

$$\varsigma_{\mathrm{AB}} = -\left(\frac{1}{3}\right)Z. \tag{66}$$

Substitution of (63), (64), and (66) into (65) yields the excitation energy as

$$\Delta E_{\text{excitation \#1}} = \varsigma'_{\mathrm{DC}} + \varsigma'_{\mathrm{CE}} - \varsigma_{\mathrm{AB}} \approx \left(\frac{1}{3}\right)Z. \tag{67}$$

It is noteworthy that the excitation energy is a positive value.

The second example is shown in Figure 22 where the electron A transfers to the orbital B at $\nu = 1/2$. The excited state #2 has two nearest electron pairs CB and BD. The excitation energy $\Delta E_{\text{excitation \#2}}$ from ground state to the state #2 is given by

$$\Delta E_{\text{excitation \#2}} = \varsigma''_{\mathrm{CB}} + \varsigma''_{\mathrm{BD}} \approx 0. \tag{68}$$

The third example is the case of $\nu = 1/4$. The hole B transfers to the orbital C and, then, the transition yields the excited state #3 as in Figure 23. Then the nearest hole pairs DC and CE are produced additionally. However, all the quantum transitions are forbidden from the hole pairs DC and CE. Accordingly the excitation energy $\Delta E_{\text{excitation \#3}}$ is zero as

$$\Delta E_{\text{excitation \#3}} = \varsigma'''^{\text{hole}}_{\mathrm{DC}} + \varsigma'''^{\text{hole}}_{\mathrm{CE}} - 2 \times \varsigma^{\text{hole}}_{\nu=1/4} = 0, \tag{69}$$

where $\varsigma^{\text{hole}}_{\nu=1/4}$ is the nearest hole pair energy. It is noteworthy that two nearest-hole pairs disappear by the excitation of the state #3. The value of $\varsigma^{\text{hole}}_{\nu=1/4}$ is zero derived from the estimation in Section 4.

Thus the excitation-energy gap has a correlation with the energy gap in the spectrum.

When the device size is very small, the ratio $\Delta y/\Delta\alpha$ becomes small. Therein, the energy gaps also become small for any fractional (not integer) filling factor. The size effect appears in a quantum Hall device with ultrasmall size (such as about 50 nm size for length ℓ).

7. Conclusion

We have developed the theory of Tao and Thouless. Then we have found the momentum conservation of the x direction for the Coulomb transitions. The momentum conservation law, Fermi-Dirac statistics, and the most uniform electron configuration produce gap structure at the filling factors $\nu = j/(2j \pm 1)$, $1/(2j+1)$, $(2j)/(2j+1)$ and gapless structure at the filling factors $\nu = 1/(2j), (2j-1)/(2j)$. Furthermore small energy gaps are estimated for examples of $\nu = 7/11$ and $4/11$ by the use of computer program. Thus, we have applied the same procedure to FQH states with arbitrary fractional filling factors, and then we have obtained various types of energy spectra for nearest electron pairs and nearest hole pairs. It is important to use the same logic for investigation of all FQH states. This paper has explained FQH states with various filling factors by using usual quantum mechanics and usual electrons without any quasiparticle.

Acknowledgments

The author would like to acknowledge Professor H. Hori and Professor K. Oto for useful discussions. The author expresses his heartfelt appreciation for the comments of the referee and the editor. This paper has been improved and revised by the comments.

References

[1] W. Pan, H. L. Stormer, D. C. Tsui, L. N. Pfeiffer, K. W. Baldwin, and K. W. West, "Transition from an electron solid to the

sequence of fractional quantum Hall states at very low Landau level filling factor," *Physical Review Letters*, vol. 88, no. 17, Article ID 176802, pp. 1–4, 2002.

[2] W. Pan, H. L. Stormer, D. C. Tsui, L. N. Pfeiffer, K. W. Baldwin, and K. W. West, "Fractional quantum hall effect of composite fermions," *Physical Review Letters*, vol. 90, no. 1, Article ID 016801, pp. 1–4, 2003.

[3] J. K. Jain, "Composite-fermion approach for the fractional quantum Hall effect," *Physical Review Letters*, vol. 63, no. 2, pp. 199–202, 1989.

[4] J. K. Jain, "Theory of the fractional quantum Hall effect," *Physical Review B*, vol. 41, no. 11, pp. 7653–7665, 1990.

[5] A. Wójs and J. J. Quinn, "Quasiparticle interactions in fractional quantum Hall systems: justification of different hierarchy schemes," *Physical Review B*, vol. 61, no. 4, pp. 2846–2854, 2000.

[6] A. Wójs, K. S. Yi, and J. J. Quinn, "Fractional quantum Hall states of clustered composite fermions," *Physical Review B*, vol. 69, no. 20, Article ID 205322, 13 pages, 2004.

[7] J. H. Smet, "Wheels within wheels," *Nature*, vol. 422, no. 6930, pp. 391–392, 2003.

[8] M. R. Peterson and J. K. Jain, "Flavor altering excitations of composite fermions," *Physical Review Letters*, vol. 93, no. 4, Article ID 046402, 4 pages, 2004.

[9] E. A. Pashitskii, "New quantum states in the fractional quantum Hall effect regime," *Low Temperature Physics*, vol. 31, no. 2, pp. 171–178, 2005.

[10] R. Tao and D. J. Thouless, "Fractional quantization of Hall conductance," *Physical Review B*, vol. 28, no. 2, pp. 1142–1144, 1983.

[11] R. Tao, "Fractional quantization of hall conductance—II," *Physical Review B*, vol. 29, no. 2, pp. 636–644, 1984.

[12] S. Sasaki, "Energy gap in fractional quantum Hall effect," *Physica B*, vol. 281-282, pp. 838–839, 2000.

[13] S. Sasaki, "Binding energy and polarization of fractional quantum Hall state," in *Proceedings of the 25th International Conference on the Physics of Semiconductors*, pp. 925–926, Springer, 2011.

[14] S. Sasaki, "Spin polarization in fractional quantum Hall effect," in *Proceedings of the 21nd European Conference on Surface Science*, vol. 532–535, pp. 567–575, June 2003.

[15] S. Sasaki, "Spin-Peierls effect in spin-polarization of fractional quantum Hall states," in *Proceedings of the 22nd European Conference on Surface Science*, vol. 566–568, pp. 1040–1046, September 2004.

[16] S. Sasaki, *Surface Science: New Research*, chapter 4, Nova Science, 2006.

[17] S. Sasaki, "Calculation of binding energies for fractional quantum Hall states with even denominators," In press, http://arxiv.org/abs/cond-mat/0703360.

[18] S. Sasaki, "Energy gaps in fractional quantum Hall states," *Journal of Physics*, vol. 100, Article ID 042021, 4 pages, 2008.

[19] S. Sasaki, "Energy spectra for fractional quantum Hall states," In press, http://arxiv.org/abs/0708.1541.

[20] S. Sasaki, "Movement of diagonal resistivity in fractional quantum Hall effect via periodic modulation of magnetic field strength," *Journal of Physics*, vol. 100, Article ID 042022, 4 pages, 2008.

[21] S. Sasaki, "Frequency dependence of diagonal resistance in fractional quantum Hall effect via periodic modulation of magnetic field," In press, http://arxiv.org/abs/0803.0615.

[22] S. Sasaki, "Consideration of ac Josephson effect in fractional quantum Hall states," In press, http://arxiv.org/abs/0807.0288.

[23] S. Sasaki, "Tunneling effect in quantum Hall device," *Journal of Surface Science and Nanotechnology*, vol. 8, pp. 121–124, 2010.